COMPREHENSIVE ROTORCRAFT AEROACOUSTICS: INVESTIGATION OF SURFACE PRESSURE DISTRIBUTION METHODS FOR ROTOR NOISE

Murat Şenipek, murat.senipek@tai.com.tr, Design Specialist
Arda Yücekayalı, ayucekayali@tai.com.tr, Loads Chief Engineer
Yüksel Ortakaya, yuksel.ortakaya@tai.com.tr, Manager of Aeronautical Sciences
Turkish Aerospace (Turkey)
Yusuf Özyörük, yusuf.ozyoruk@ae.metu.edu.tr, Professor, Middle East Technical University (Turkey)

Abstract
Having full helicopter trim capability, comprehensive codes are indispensable for helicopter aeromechanics yet they operate over spanwise concentrated aerodynamic loads calculated at blade segment aerodynamic centers. In this study, an approach to generate distributed aerodynamic loads from comprehensive models, over real blade geometry for further aeroacoustic calculations of a helicopter rotor is proposed. Distribution of concentrated aerodynamic loads over upper and lower surface of the blade geometry with the help of an airfoil pressure database to prepare higher resolution data for acoustic solvers is studied. In order to assess the improvement, first, the concentrated aerodynamic loads are distributed over two-dimensional representative upper and lower surfaces then over three-dimensional blade geometry and acoustic signatures are compared with each other, HART-II wind tunnel test data and benchmark tool PSU-WOPWOP.

1. INTRODUCTION

Aeroacoustics signature for a helicopter rotor is an overall outcome of coupled aerodynamic, dynamic and aero-elastic response of the blades. This multi-disciplinary nature of the helicopter rotor requires a comprehensive analysis to predict accurately noise characteristics. There are numerous commercial and in-house developed comprehensive analysis codes for rotorcrafts available with varying levels of fidelity. Generally, blade surface-pressure distribution is not the concern of the comprehensive codes except limited number of concentrated loads distributed over the chord line. On the contrary, majority of the rotor-noise analysis tools utilize integral formulation of Ffowcs Williams-Hawkings equation, which requires time dependent blade surface-pressure distribution [1], [2].

Although computational fluid dynamics (CFD) approaches provide detailed pressure distribution on the real blade geometry, full helicopter trim including rotor dynamics and aero-elastic response requires high fidelity CFD-CSD solution, which is computationally expensive and still not practical to utilize in the preliminary design loop [3]. Therefore, comprehensive tools such as CAMRAD II and CHARM required to be coupled with an acoustic solver to predict rotorcraft noise. As typically, comprehensive codes operate over concentrated aerodynamic load points or 2-D vortex lattice sheets without segregating upper and lower surfaces of the rotor blade, they lack in generating accurate pressure distribution over the 3-D blade surface. Therefore, a methodology to generate required blade pressure data is essential so that more accurate aero-acoustic predictions can be obtained.

In this study, different approaches are studied and assessed to project concentrated aerodynamic loading over the blade geometry and their effects on acoustic pressure are investigated. A direct upper & lower surface decomposition and utilization of airfoil pressure distribution interpolation are considered.

Aerodynamic loading is obtained by CHARM, commercial comprehensive rotorcraft analysis software. Loading on the blades are calculated by Vortex-Lattice-Methodology (VLM) and Lifting Line Theory (LLT). VLM incorporates sectional 2-D airfoil aerodynamic coefficient tables by using their lift curve slope to calculate sectional angle of attack and uses drag and moment coefficients accordingly. On the other hand, LLT provides a spanwise bound vortex system to calculate local angle of attack and uses airfoil tables to find the local lift coefficient. Both methodologies calculate the rotor wake and flowfield around the rotor so that loading, thickness and BVI noise estimations can be performed by using a proper blade pressure distribution. After providing an unsteady pressure distribution on rotor blades aeroacoustics calculations are performed by TACO

Presented at 45th European Rotorcraft Forum, Warsaw, Poland, 17-20 September, 2019

(Turkish Aerospace Acoustic Code), which integrates Ffowcs Williams-Hawkings equation using either retarded or advance time algorithms to calculate aerodynamic pressure fluctuations and noise levels at given observer locations [3]. Previous studies with TACO showed well prediction of rotor noise requires accurate blade aerodynamic loading [3]. The interface between CHARM and TACO is constituted with a pre/post-processor, which utilizes concentrated blade loadings and generates blade surface-pressure distribution. The main purpose of this work is to assess the sensitivity of 3-D pressure distribution methods to improve aeroacoustics evaluations performed over comprehensive codes and minimize the discrepancy between comprehensive tools and CFD analyses. Effects of utilizing proper pressure distribution over 3-D geometry instead of concentrated loads generated by comprehensive codes are studied. Feasibility of the implemented methodology in terms of accuracy and computational cost is investigated.

Results for various pressure projection approaches are discussed in terms of accuracy, aeroacoustics characteristics and sensitivity. Experimental data HART II test campaign is used, and each methodology is compared with the test data.

2. METHOD

In general, blade loading is calculated from 2-D (M, α) sectional data or simply lift curve slope which do not include information about the chordwise distribution of pressure varying under angle of attack and Mach number effects. Lift curve slope-based formulations are also do not consider post stall behaviour of the chordwise pressure distribution. Although chordwise aerodynamic loading distribution can be generated by representing blades with 2-D Vortex Lattice Method (VLM) surfaces or spanwise distributed vortex system (LLT) with a post-process in CHARM as given in Figure 1. Furthermore, it is experienced that distribution of blade pressure in 3-D (i.e. upper and lower surfaces) is highly crucial when dimensions of advanced blade tips and interested aeroacoustics frequencies are considered. Therefore, approximating the pressure distribution for upper and lower sections of the blade and projecting them onto real or simplified blade geometry is essential to estimate directivity characteristics, frequency spectra and total aeroacoustics noise level accurately.

In VLM bound circulation is modeled with vortex lattice quadrilaterals whose strengths satisfy tangent flow at panel control points. 2-D look-up tables are used to determine profile drag, pitching moment and zero lift angle of attack. Lift curve slope required for VLM calculations are estimated from 2-D airfoil tables therefore this methodology lacks the post stall behavior and real 2-D airfoil lift coefficient data.

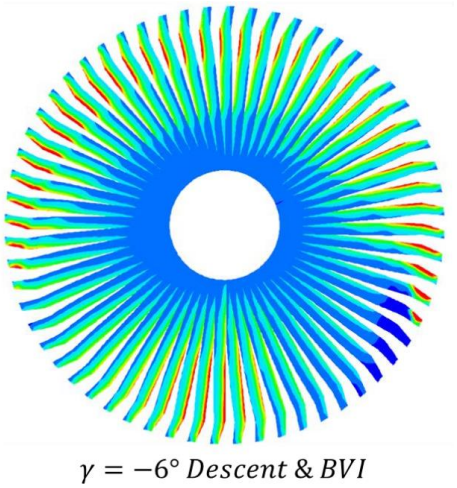

Figure 1 Time dependent pressure distribution of a rotor disk with BVI (top view)

Aerodynamic loads are calculated by CHARM for trimmed flight that provides concentrated loading with time on the blade in a 2-D grid or span-wise 1-D aerodynamic collocation points. CHARM calculates chordwise distribution of aerodynamic loading by VLM at a limited number of collocation points, which provides a consistent loading with 2-D viscous aerodynamic data as represented in Figure 5 (left and middle). Blade pressure distribution is obtained as net pressure on the VLM sheets instead of separated upper and lower surface pressures. Therefore, the VLM sheets do not represent the real blade geometry but represents the chord, twist, sweep and anhedral distribution.

Another option in CHARM is the utilization of LLT and/or second order LLT that represents lift distribution over the blade. In this case local angle of attack is calculated by LLT and it is an input to airfoil coefficient database and C_l is the output. Therefore, post stall characteristics and nonlinear regions in the lift curve may be captured. In VLM the local angle of attack is the output of the vortex system and drag and moment coefficients are calculated accordingly. Due to this difference, both methodologies are investigated in terms of rotor BVI related aeroacoustics and it is aimed to decrease the discrepancy between two methodologies.

The flow chart for the proposed acoustic analysis procedure is depicted with Figure 2. Methodology starts with a comprehensive rotor analysis for a given flight and/or trim condition. Then, previously generated pressure databases are imported to approximate the spanwise and chordwise pressure distribution of the rotor blade for the full revolution.

All geometry details such as blade twist, sweep, anhedral and taper are taken into account while performing the pressure interpolation. Pre-process part requires time dependent angle of attack and Mach number for each blade element.

Presented at 45th European Rotorcraft Forum, Warsaw, Poland, 17-20 September, 2019

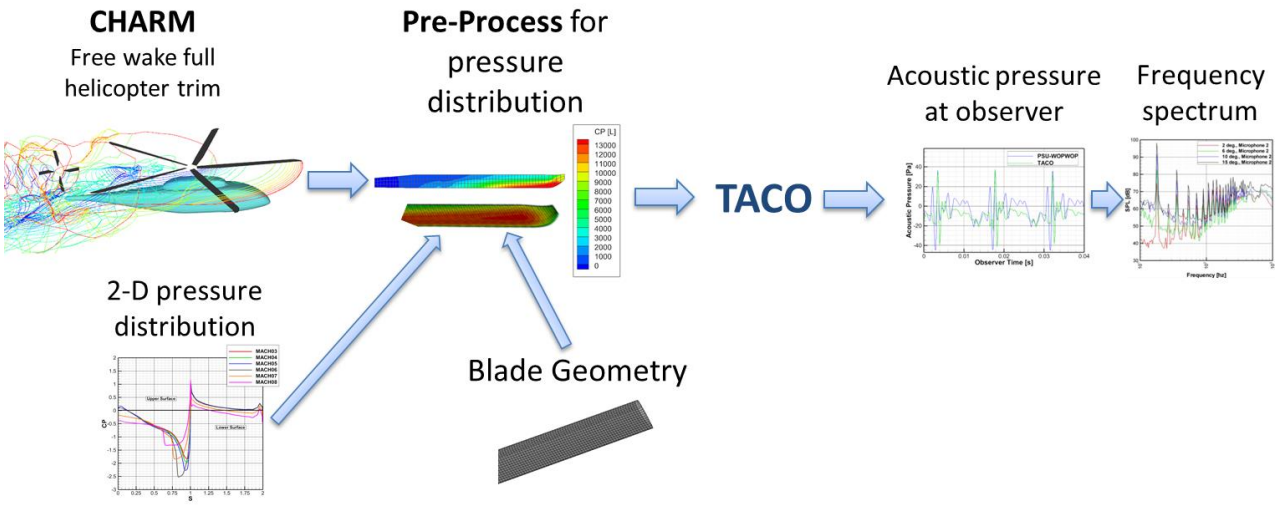

Figure 2 Proposed Aeroacoustics Analysis Methodology

Sample effective angle of attack and Mach number variation along the rotor disk is obtained as illustrated with Figure 3 and Figure 4. After required input files are generated TACO analyses are performed to obtain acoustic pressure levels at an observation point and frequency spectrum data of the rotor noise.

In the proposed methodology, pressure variation belonging to each analysed airfoil is stored in a database for varying angle of attack and Mach number together with the airfoil surface coordinates. By using the airfoil coordinates, 3-D geometry is generated and pressure distribution can be obtained for any given α and M combination. Furthermore, azimuth-wise interpolation is available to increase the fidelity of time dependent rotor blade pressure. However, intermediate level phenomenon cannot be captured by interpolation. Therefore, it may be necessary to increase not only the interpolated azimuth-wise discretization but also the analysis fidelity.

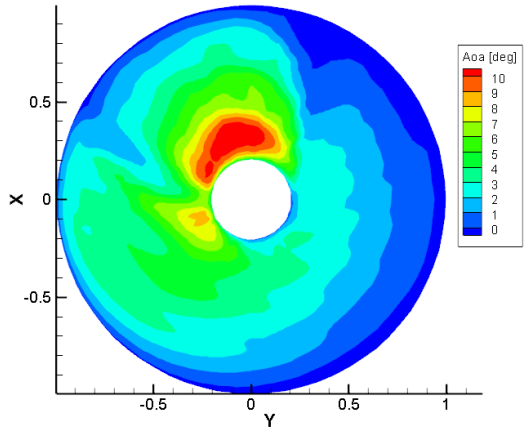

Figure 3 Rotor disk α distribution V_∞ (along –x)

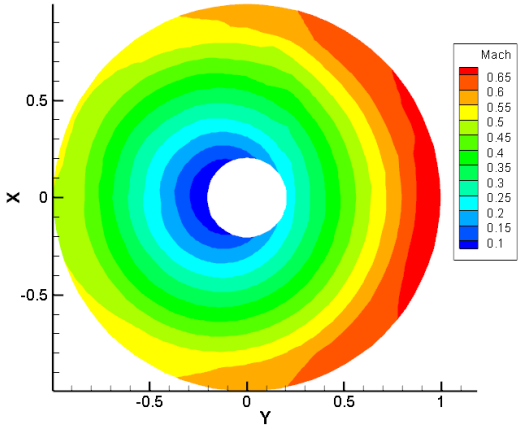

Figure 4 Rotor disk Mach distribution V_∞ (along –x)

The single sheet pressure/loading data is then separated as upper and lower surfaces as illustrated in Figure 5 (right) to represent upper and lower surfaces. As a simplified 3-D geometry representation, two sheets are generated at a mean thickness distance to separate the pressure to upper and lower surfaces. These surfaces are generated by using the pressure output file of CHARM code which generates net pressure difference between the lower and upper surfaces of the blade by using VLM. Generation of surfaces, defining the upper and lower surfaces and defining the weight of the distribution is performed within the pre-process code before TACO analyses. Connectivity information is arranged so that surface unit normal points outwards from the vortex sheet as given in Figure 5 (right). In conclusion, vortex sheet distribution methodology directly uses and manipulates the pressure output file obtained from CHARM.

Presented at 45th European Rotorcraft Forum, Warsaw, Poland, 17-20 September, 2019

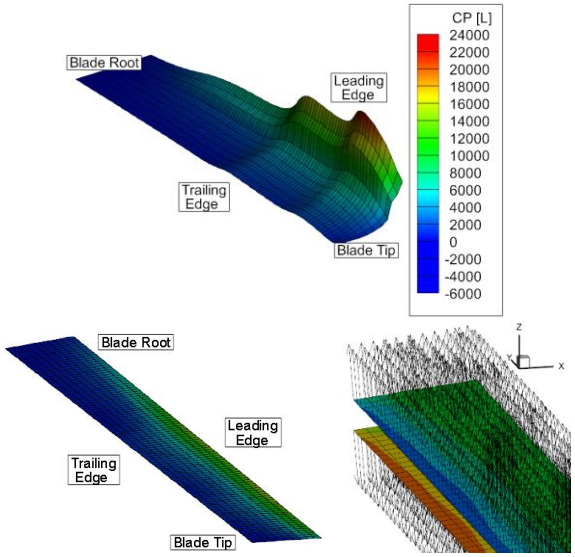

Figure 5 Sample pressure distribution for advancing blade (up), sheet model pressure distribution (left) and seperated upper and lower VLM surface panels (right)

As the main motivation of this study, the use of two dimensional airfoil pressure-distribution values for chordwise pressure distribution and interpolating each section to the 3-D blade geometry is studied. Since 2-D airfoil data is previously generated by CFD solvers to be imported by CHARM, chordwise pressure distribution data is available and easy to store in a database for further use. This chordwise pressure distribution is available for full angle of attack (α) and Mach number (M) envelope whose boundaries are extending from -180° to +180° α and up to 1.0 Mach. Therefore, the available pressure distribution values cover post stall angles of attack, compressible and transonic flow regions. This data enables to interpolate the pressure distribution on any section of the rotating blade for desired α and Mach number values. In this approach, the effects that are caused by 3-D flow on the rotor blades such as shock delay, stall delay, yawed flow and dynamic stall are neglected. However, rotational effects on the blade do not generate dramatic difference in pressure field as stated by Heller [8].

In this study, the sensitivity of the blade surface distribution on acoustic pressure levels is of interest, therefore 3-D blade geometry is integrated to the post process code that manipulates the CHARM data and generates time dependent pressure input set into TACO code. The purpose is to approximate a realistic pressure field on the rotor blade by making use of previously generated 2-D viscous sectional information. Several approximations to represent the chordwise pressure distribution as triangular or piecewise linear functions provided in the literature [6]. However, pressure variation with Mach number illustrated in Figure 6 shows that the upper surface pressure field is stronger than the lower surface at zero angle of attack.

Therefore, it is evaluated that the methodology should represent upper and lower surface pressure details instead of focusing on the net pressure distribution.

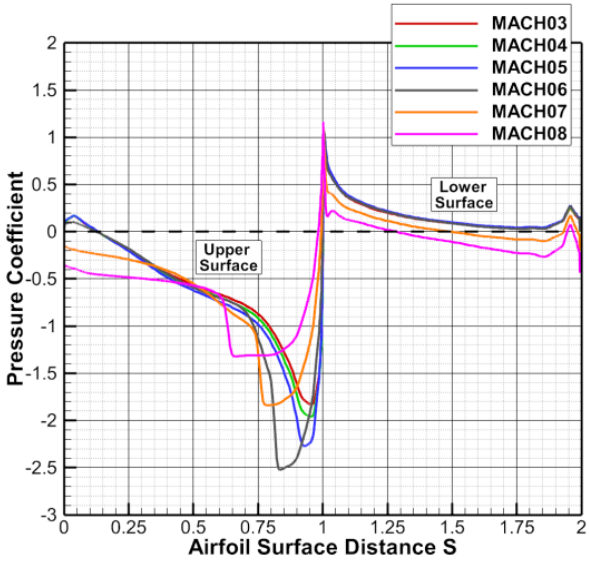

Figure 6 Airfoil Cp distribution with Mach number

Then 2-D pressure distributions related with instantaneous angle of attack and Mach number are distributed over the blade planform as illustrated with Figure 7. Blade pressure distribution is interpolated from 2-D airfoil pressure variation over 3-D real blade geometry as illustrated with Figure 8

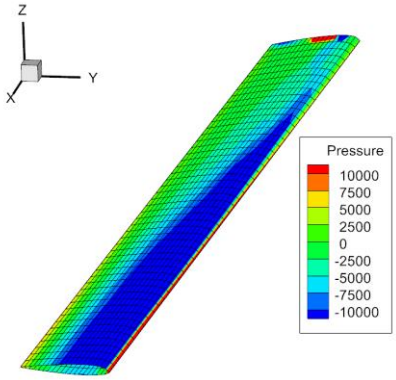

Figure 7 Blade pressure distribution

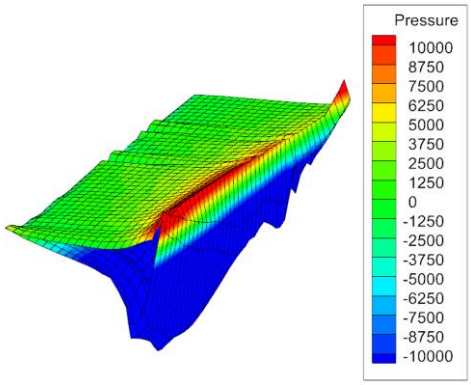

Figure 8 Chordwise pressure variation illustrated over 3-D blade geometry

Presented at 45th European Rotorcraft Forum, Warsaw, Poland, 17-20 September, 2019

3-D blade geometry with pressure distribution varying with time and all surface normal out pointing of the surface as demonstrated with Figure 9 are then supplied to the acoustic solver TACO for further noise calculations.

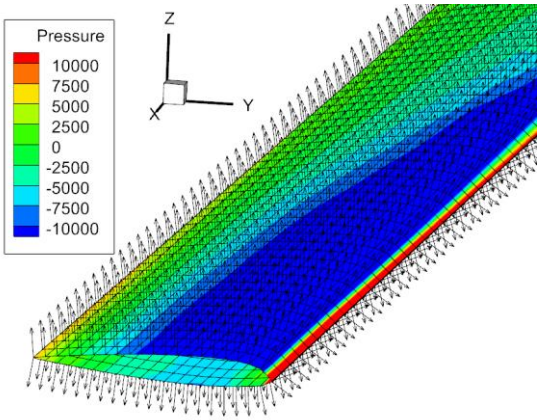

Figure 9 Surface normals and pressure distribution

In this study, spanwise concentrated loads are determined with VLM and LLT approaches and effects on accuracy are studied for single sheet, double sheet and pressure interpolation methods for comprehensive analyses tools to predict the rotor noise. Sensitivity analyses in terms of azimuth-steps, spanwise and chordwise discretization fidelity is performed and results are discussed.

3. RESULTS & DISCUSSION

In this work, HART-II rotor is modelled and microphones are located according to the experiments performed [4]. HART-II rotor is a scaled version of BO-105 helicopter rotor having rectangular geometry with 2m tip radius, -8° linear twist and rotating at 1041 rpm as given in Table 1. Analysed case belongs to BL case having 0.15 advance ratio at 4.5° effective shaft angle of attack (α_s) which is a kind of BVI descent condition.

Table 1 HART-II Wind tunnel test rotor model

Specifications	Values
Blade Span	2m
Rotational Speed	1041 rpm
Blade Twist	-8° linear
Precone Angle	2.5°
Root cut out	22 %
Number of blades	4

CHARM analyses are performed at the same conditions for several settings and models to investigate the blade pressure distribution effects on the BVI rotor noise. Figure 10 shows the rotor wake and vortex filaments of HART-II rotor for BL test case.

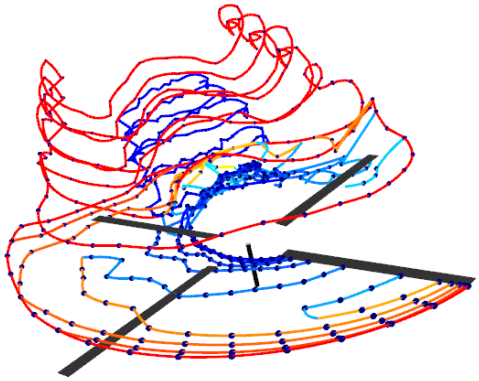

Figure 10 CHARM HART II Rotor Wake for BL $\alpha_s = 4.5°$

Blade surface pressure is obtained for BO-105 main rotor by CHARM to compare with the aeroacoustic test data from HART II. Single sheet, double sheet with equal distribution and asymmetric distribution of pressure coefficients, and geometry pressure distribution methods are applied on the generated surfaces and analyzed by TACO to investigate the sensitivity of the acoustic pressure levels from the experimental data.

3.1. Vortex Sheet Models

Vortex sheets are obtained as previously shown in Figure 1 and Figure 5. Firstly, single faced sheet is used to calculate rotor noise for microphone 11 which is located below the advancing side of the rotor. Single faced sheet acoustic pressure levels are provided in Figure 11 and shows acceptable amount of consistency with the test. However, peak to peak values of acoustic pressure is lower than the test.

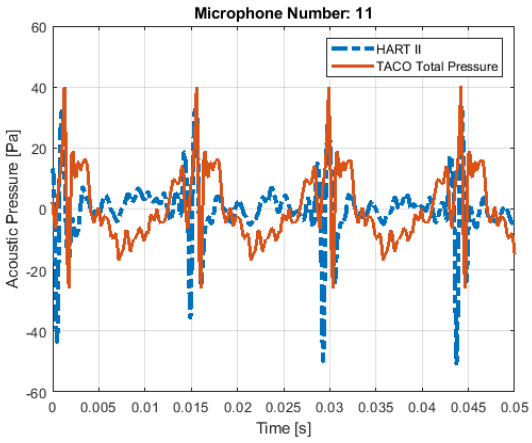

Figure 11 Single sheet pressure distribution comparison with test data for 360 azimuth steps (1°/step)

In Figure 12, Figure 13 and Figure 14 double sheet pressure distribution is performed on the rotor blades to separate the lower and upper side of the blade. Upper and lower sides have symmetric and asymmetric pressure distribution levels that provide the identical total pressure when integrated with the CHARM result.

Presented at 45th European Rotorcraft Forum, Warsaw, Poland, 17-20 September, 2019

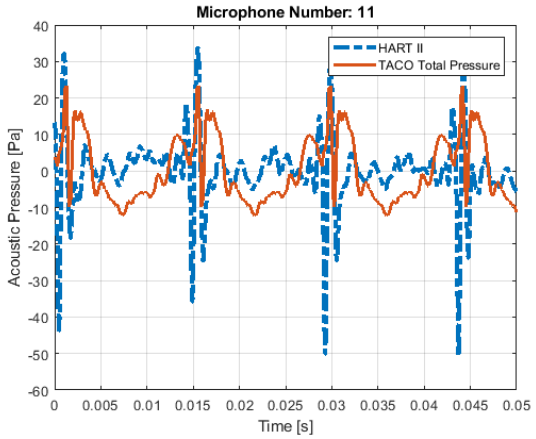

Figure 12 Symmetric single sheet pressure distribution for 360 azimuth steps (1°/step)

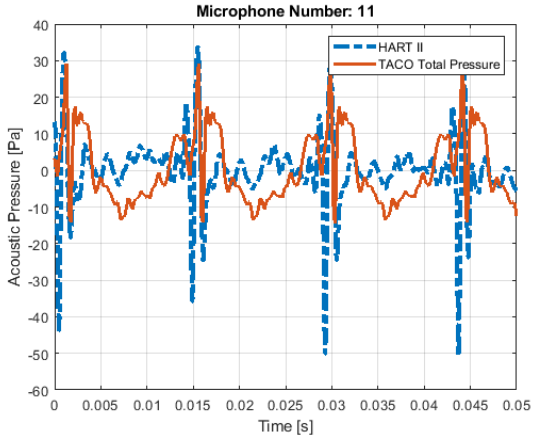

Figure 13 Asymmetric 1/3 upper side pressure distribution for 360 azimuth steps (1°/step)

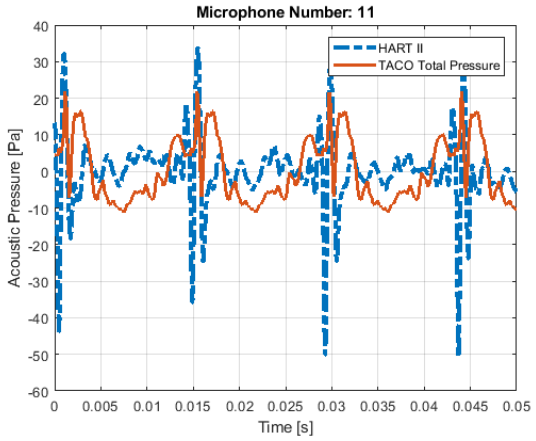

Figure 14 Asymmetric 2/3 upper side pressure distribution for 360 azimuth steps (1°/step)

In this part, all sheet pressure distributions have 1° of resolution in time that corresponds 360 data points for a rotor revolution. Symmetric and asymmetric pressure sheet models provide similar noise characteristics and underestimates the BVI related noise when compared with the test data. Identical analysis condition and rotor wake is used for the geometry pressure distribution model to compare the results.

3.2. Geometry Pressure Distribution Models

In geometry distribution methods, local angle of attack and Mach number distributions are used to interpolate the airfoil pressure distribution as provided in Figure 15. However, the problem in this methodology is that CHARM cannot provide local α and M for high resolution. It reconstructs the rotor wake to provide VLM calculated pressure distribution (which is used in previous methodology) in 360 or 540 azimuth steps, but did not provide the angle of attack distribution at the same fidelity. The maximum azimuth steps for α output is 240 which significantly increases the time to converge a solution. Therefore, different methodologies are investigated to observe the effects on the rotor noise. Firstly, an interpolation procedure is performed to increase the number of samples as a post process. Then, azimuth resolution is increased up to 240. Finally, the resolution is increased up to 960 (i.e. 0.375°/step) to observe the effects on the rotor noise.

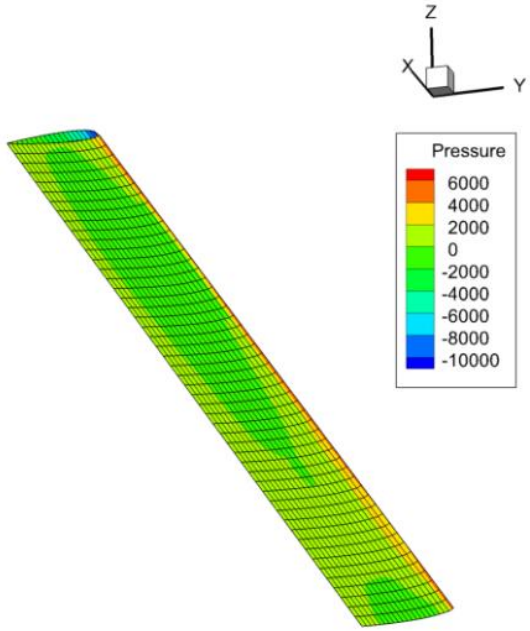

Figure 15 Geometry with pressure distribution from bottom view

In Figure 16, Figure 17, Figure 18, and Figure 19 different azimuth-wise discretization are performed as 36,72,144 and 240. All charm results are interpolated to provide 1° resolution of the rotor blade motion to preserve the consistency with the results in the pressure sheet methodology. All rotor blades have 20x100 rectangular grid. It is observed that with the increase in azimuth-wise resolution, the results converge close to the test predictions. However, it is evaluated that 240 steps solution still needs increased azimuth-wise resolution to capture the BVI related acoustic pressure.

Presented at 45th European Rotorcraft Forum, Warsaw, Poland, 17-20 September, 2019

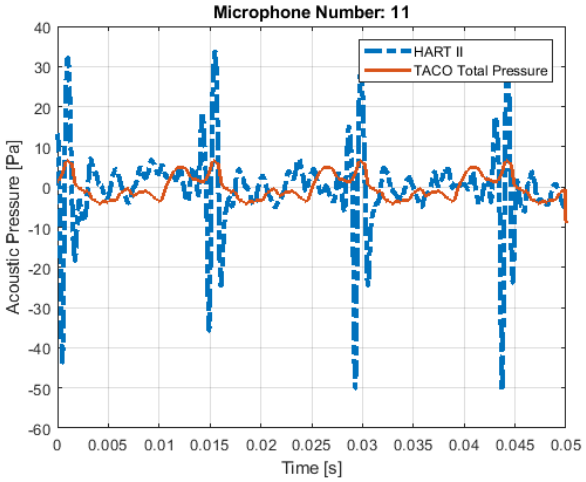

Figure 16 VLM solution with 36 azimuth steps interpolated to 360 (1°/step)

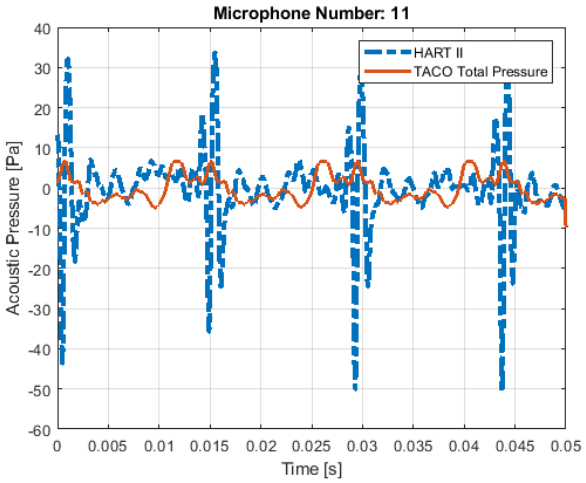

Figure 17 VLM solution with 72 azimuth steps interpolated to 360 (1°/step)

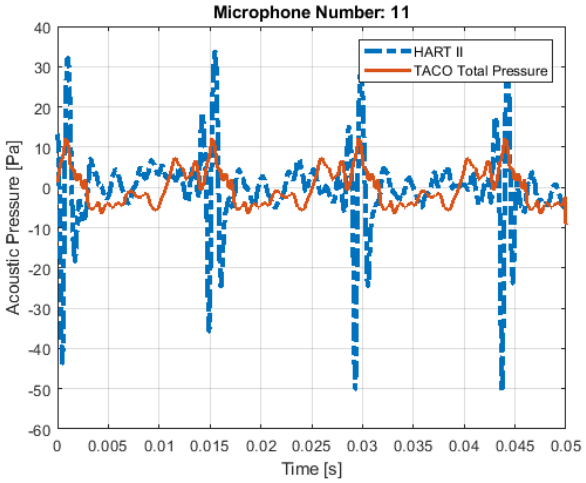

Figure 18 VLM solution with 144 azimuth steps interpolated to 360 (1°/step)

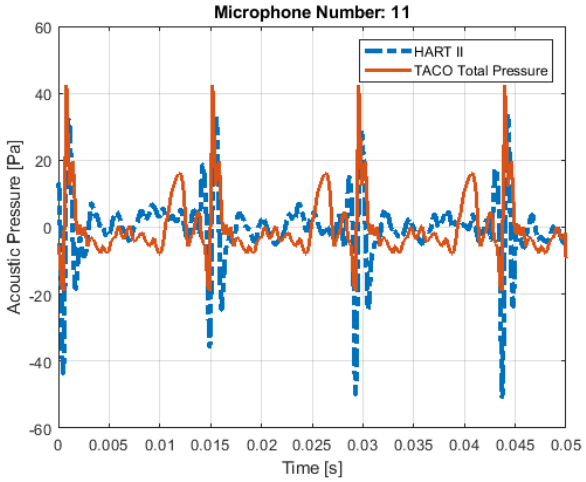

Figure 19 VLM solution with 240 azimuth steps interpolated to 360 (1°/step)

VLM solution having 240 azimuth steps is interpolated to 960 azimuth steps (0.375°/step) to observe the results and peak-to-peak pressure levels becomes close to the test results. Noting that the all analyses results belongs to the identical trim condition and only the azimuth-wise time step parameter is changed.

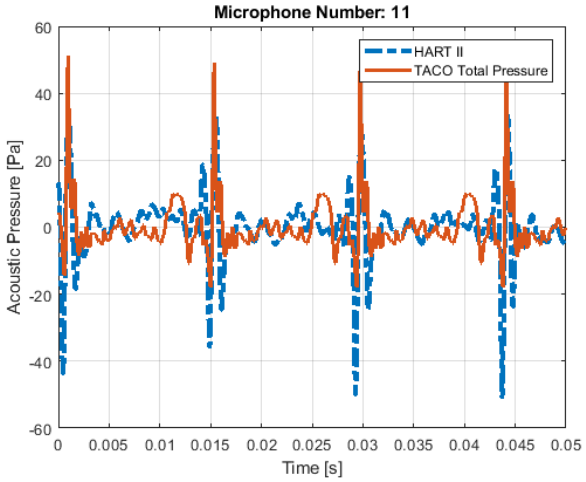

Figure 20 VLM solution with 240 azimuth steps interpolated to 960 (0.375°/step)

Detailed comparison is performed in Figure 21 and it can be observed that as the number of azimuth-wise discretization is increased, BVI related noise characteristics can be captured. Peak to peak value of analysis pressure levels is about 67 Pa where the test result is about 69 Pa.

Presented at 45th European Rotorcraft Forum, Warsaw, Poland, 17-20 September, 2019

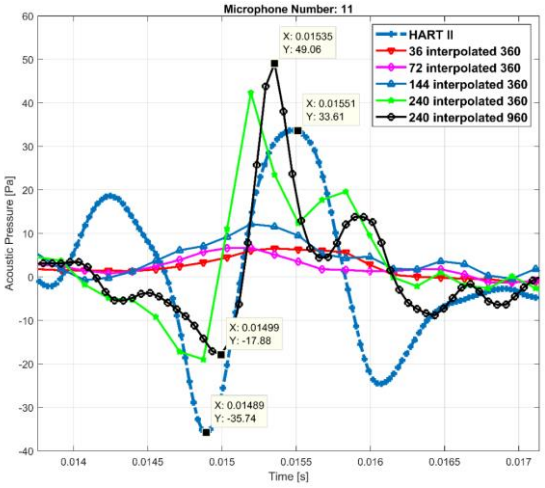

Figure 21 Comparison of azimuth-wise discretization effect over aeroacoustic pressure

The same analysis condition is analysed by using LLT to compare between the two methodologies. Aeroacoustic analysis result is provided in Figure 22; however, there is no BVI related impulsive noise. In the analysed case BVI phenomenon could not be captured by using LLT.

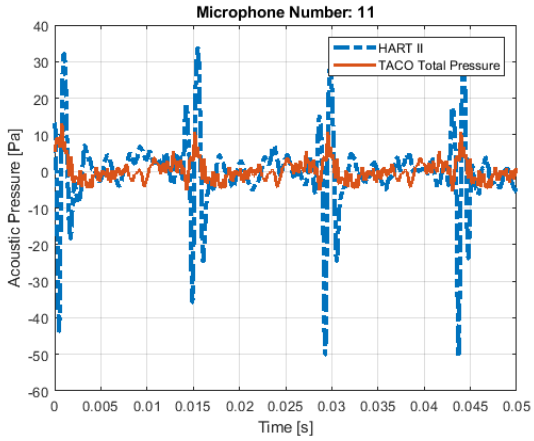

Figure 22 LLT solution with 240 azimuth steps interpolated to 960 (0.375°/step)

In order to observe the BVI related changes in aerodynamic loading, disk plots are generated for different spanwise analysis azimuth steps as illustrated in Figure 23, Figure 24, Figure 25, and Figure 26. Azimuth steps are determined as 36, 72, 144, and 240 respectively. As the number of azimuth-wise resolution increases BVI related change of blade loading is captured more precisely that is clearly seen in Figure 26. Although the highest resolution is applied to the solution with LLT, BVI related blade loading formations disappear. That is the main reason for the acoustic pressure prediction of LLT as previously shown in Figure 22.

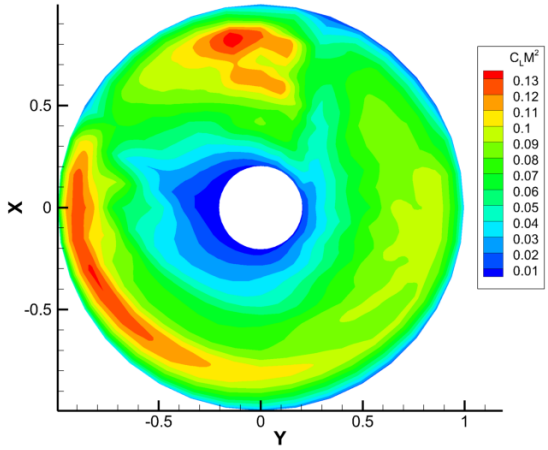

Figure 23 Disk contours of C_LM^2 for VLM solution with 36 azimuth steps interpolated to 360 (1°/step)

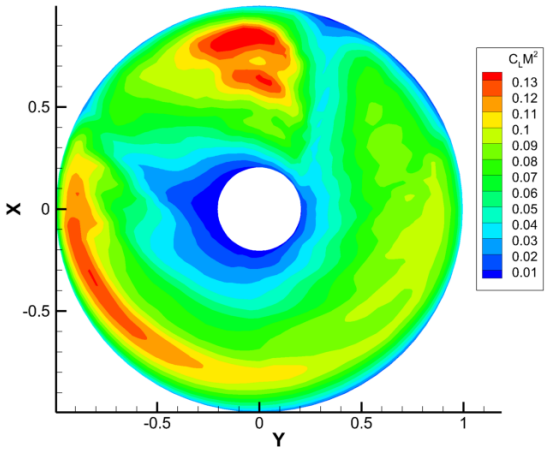

Figure 24 Disk contours of C_LM^2 for VLM solution with 72 azimuth steps interpolated to 360 (1°/step)

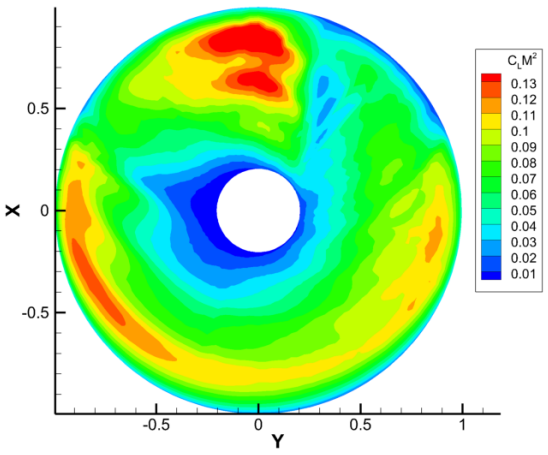

Figure 25 Disk contours of C_LM^2 for VLM solution with 144 azimuth steps interpolated to 360 (1°/step)

Presented at 45th European Rotorcraft Forum, Warsaw, Poland, 17-20 September, 2019

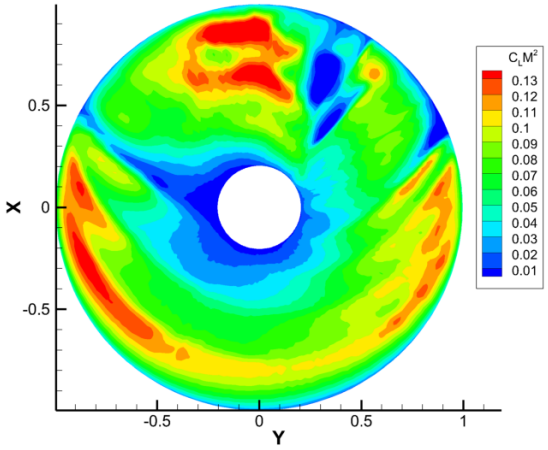

Figure 26 Disk contours of $C_L M^2$ for VLM solution with 240 azimuth steps interpolated to 360 (1°/step)

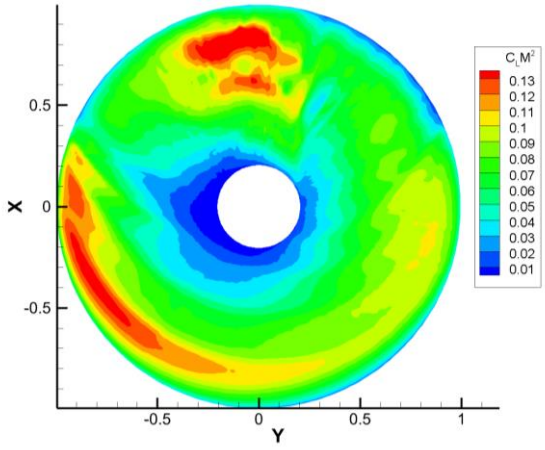

Figure 27 Disk contours of $C_L M^2$ for LLT solution with 36 azimuth steps interpolated to 360 (1°/step)

Sensitivity analyses are performed for different chordwise and spanwise number of cells to compare the sensitivity of the BVI related noise. Above analyses are performed for 20x100 grid and reasonable results are obtained. Similar analysis result is obtained with 40x50 grid with a validated VLM scheme in order to provide more chordwise cells to reflect a higher fidelity pressure distribution as illustrated in Figure 28. However, decreasing the number of spanwise cells reduces the fidelity of the BVI related change in angle of attack and local Mach number.

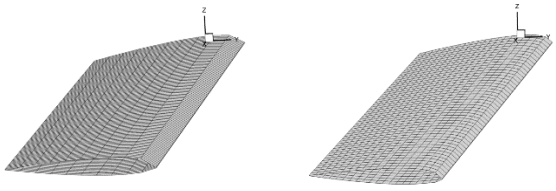

Figure 28 VLM 20x100 (left) and 40x50 (right) blade grids

Results obtained for 40x50 grid is provided in Figure 29. Analysis does not show any consistency with the test data and when compared with the similar case in Figure 19 (20x100), and the accuracy of the analysis is reduced significantly. Therefore, it is observed that the number of spanwise cells is as critical as azimuth-wise resolution of the blade motion.

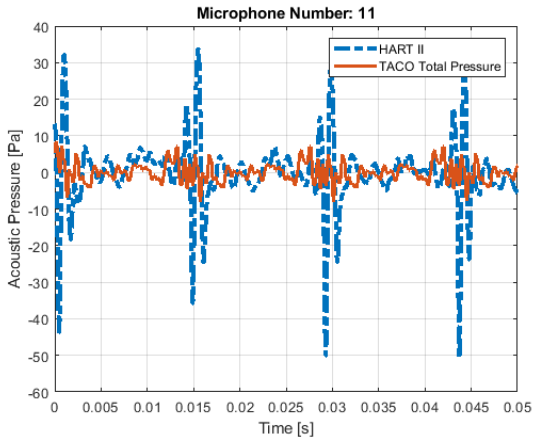

Figure 29 VLM solution with 240 azimuth steps interpolated to 360 (1°/step) with 40x50 grid size

Thickness Noise Prediction

Prediction of thickness noise values for two methods show difference as given in Figure 30 and Figure 31. Since there is not a realistic 3-D geometry in sheet models, the thickness acoustic pressure waves are calculated too large to be realistic about 30 Pa peak-to-peak values. The main reason of this result is that sheet models generate monopole source and sink perpendicular to the chordline. In fact, it is anticipated that there will be more realistic thickness noise due to the perpendicular unit normals on the realistic 3-D geometry model with a proper pressure distribution along the sectional blade profiles. Thickness related acoustic pressure for the 3-D geometry models are predicted about 5 Pa peak-to-peak values.

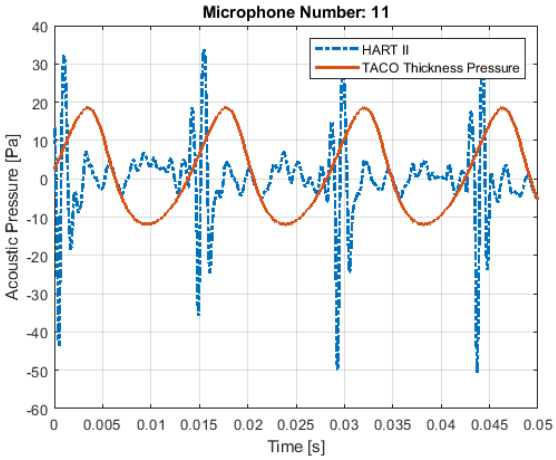

Figure 30 Sheet methods thickness noise

Presented at 45th European Rotorcraft Forum, Warsaw, Poland, 17-20 September, 2019

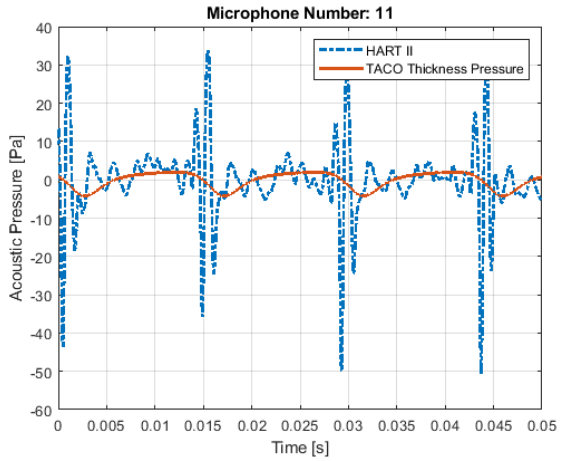

Figure 31 Geometry methods Thickness noise

Comparison with a benchmark tool PSU-WOPWOP is performed and result is given in Figure 32. Aeroacoustic pressure levels provides similar results and the small difference is caused by the blade surface processing approaches of the two tools.

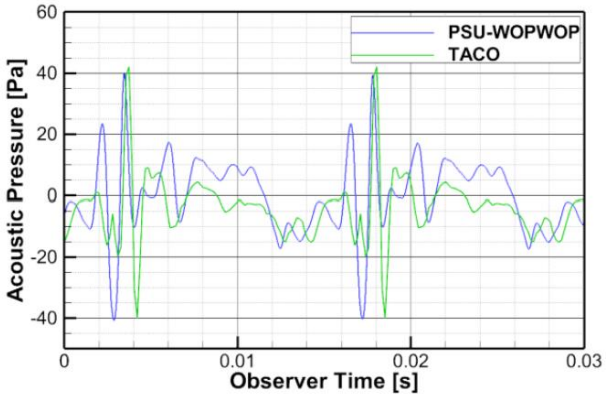

Figure 32 TACO vs. PSU-WOPWOP comparison [5]

4. CONCLUSION

In this work the interface between CHARM and TACO has been developed to use the comprehensive analysis methods while predicting the rotor noise. Results with upper and lower surface decomposition approaches have been obtained. Airfoil pressure database has been generated and acoustic analyses with pressure distribution projected over 3-D real geometry is performed. Acoustic pressure variation has been calculated and compared with HART-II test data. Following conclusions are made during the investigation of surface pressure distribution methods:

- Since BVI is an impulsive noise, the dynamics od BVI is fast. Therefore, it requires high resolution in azimuth steps and spanwise discretization to capture the acoustic pressure.
- Sheet methods are suitable for tuning and promising noise calculation results might be obtained after some tuning.
- 3-D geometry pressure distribution methodology highly depends on the fidelity. Increment in the fidelity of the rotor wake and the solution leads to an increased accuracy. Therefore, this methodology is applicable any type of high fidelity solution providing time dependent local α and Mach number. This methodology is promising when applied with higher fidelity rotor wake analyses methods such as Viscous Vortex Particle Methods (VVPM).
- With the increasing resolution, it is observed that the BVI frontends increase in loading contour plots. Therefore, more accurate BVI noise predictions are performed.
- Further work is required to be performed on the 3-D distribution approach including the comparison with the CFD solutions.
- Comparison with rotor wake solutions by using VVPM may be performed as a future work. In VPM, unsteady, high fidelity rotor wake, and rollup vorticity is calculated naturally. Therefore, it is evaluated as suitable for comprehensive rotor aeroacoustics.

5. REFERENCES

[1] Brentner S. K., “PSU-WOPWOP User’s Guide”, Pennsylvania State University, February 2, 2014.

[2] Brentner, S. K., Farassat, F., “Modeling Aerodynamically Generated Sound of Helicopter Rotors”, Progress in Aerospace Sciences.

[3] Özyörük, Yusuf, Ali Ünal, and Ali Oğuz Yüksel. "Noise predictions of helicopter rotors in hover and forward flight." AIAA/CEAS Aeroacoustics Conference. Denver, 2017.

[4] Yung H. Yu, Tung C., Wall V. van der, et. al., The HART-II Test: Rotor Wakes and Aeroacoustics with Higher-Harmonic Pitch Control (HHC) Inputs - The Joint German/French/Dutch/US Project – AHS 58th Annual Forum, 2002, Montreal, Canada

[5] Yücekayalı, Arda, Murat Şenipek, Yüksel Ortakaya, and Yusuf Özyörük. "Main and Tail Rotor Full Helicopter Trim Noise Predictions." 7th Asian/Australian Rotorcraft Forum. Jeju Island, Korea, 2018.

[6] Dobrev I, F Massouh, and M Rapin. "Actuator surface hybrid model." Journal of Physics: Conference Series 75 75 (2007).

[7] Gray, R. B., H. M. McMahon, K. R. Shenoy, and L. M. Hammer. Surface Pressure Measurements at two tips of a Model Helicopter Rotors in Hover. NASA, n.d.

[8] Heller, H., H. Buchholz, K. J. Schultx, S. R. Ahmed, and W. Splettstoesser. "Helicopter Rotor Blade Aeroacoustics: A Comparison of Model-Scale Wind Tunnel and Full-Scale Flight Test Results." ICAS. 1996.

Presented at 45th European Rotorcraft Forum, Warsaw, Poland, 17-20 September, 2019